Dynamic Restoration Mechanisms in Al-5.8 At. Pct Mg Deformed to Large Strains in the Solute Drag Regime

G.A. HENSHALL, M.E. KASSNER, and H.J. McQUEEN

An Al-5.8 at. pct Mg (5.2 wt pct Mg) alloy was deformed in torsion within the solute drag regime to various strains, up to the failure strain of 10.8. Optical microscopy (OM) and transmission electron microscopy (TEM) were used to analyze the evolution of the microstructure and to determine the dynamic restoration mechanism. Transmission electron microscopy revealed that subgrain formation is sluggish but that subgrains eventually ($\bar{\varepsilon} \approx 1$) fill the grains. The "steady-state" subgrain size ($\lambda \approx 6\ \mu m$) and misorientation angle ($\Theta \approx 1.6$ deg) are reached by $\bar{\varepsilon} \approx 2$. These observations confirm that subgrains eventually form during deformation in the solute drag regime, though they do not appear to significantly influence the strength. At low strains, nearly all of the boundaries form by dislocation reaction and are low angle ($\Theta < 10$ deg). At a strain of 10.8, however, the boundary misorientation histogram is bimodal, with nearly 25 pct of the boundaries having high angles due to their ancestry in the original grain boundaries. This is consistent with OM observations of the elongation and thinning of the original grains as they spiral around the torsion axis. No evidence was found for *discontinuous* dynamic recrystallization, a repeating process in which strain-free grains nucleate, grow, deform, and give rise to new nuclei. It is concluded that dynamic recovery in the solute drag regime gives rise to *geometric* dynamic recrystallization in a manner very similar to that already established for pure aluminum, suggesting that geometric dynamic recrystallization may occur generally in materials with a high stacking-fault energy (SFE) deformed to large strains.

I. INTRODUCTION

ELEVATED-temperature torsion tests have been used to study the dynamic restoration mechanism in an Al-5.8 at. pct Mg alloy deformed in the solute drag regime. The major goal was to determine whether the mechanical and microstructural changes that occur in this alloy at large strains are caused by discontinuous dynamic recrystallization or by a recovery-controlled mechanism with concomitant geometric dynamic recrystallization (defined below). Therefore, this work was a continuation of earlier work on pure aluminum published in this journal by one of the authors.[1,2] In these previous investigations, techniques similar to those employed in the present study were used to establish that dynamic restoration in pure Al occurs through dynamic recovery with concomitant geometric dynamic recrystallization. The current work was undertaken to test whether this mechanism also accounts for the dynamic restoration behavior of an Al-Mg alloy deformed in the viscous solute drag regime.

The extremely large ductility of pure aluminum under warm- and hot-working conditions in torsion is due to the high level of dynamic recovery which, in turn, is largely the consequence of the high stacking-fault energy (SFE).[3-8] Studies[1-8] have shown that the propensity for dynamic recovery in pure Al is so great that *discontinuous* dynamic recrystallization, a repeating process in which strain-free grains nucleate, grow, deform, and give rise to new nuclei, does not occur. The dynamic recovery does not appear to allow the formation of regions of high dislocation density that lead to the nucleation and subsequent growth of new strain-free grains, which are often observed in low SFE metals and alloys.[9,10]

At very high strains, a process occurs in pure Al that was termed by McQueen and co-workers as *geometric* dynamic recrystallization[6,7,8] and is associated with extensive dynamic recovery. Briefly, at low strains, equiaxed subgrains begin to form and the high angle grain boundaries become serrated due to boundary migration at junctions with the subgrain boundaries. By strains of about 0.5, the subgrains in pure Al reach a "steady-state" size and the boundaries formed by dislocation reaction reach an average misorientation angle that does not change substantially with increasing strain.[1,4] (The saturation of misorientation angle with strain for these boundaries provides evidence that dynamic restoration in pure Al does not occur through a *continuous* dynamic recrystallization mechanism, in which the misorientation angle between subgrains continuously increases to the point that the misorientation becomes typical of high-angle grain boundaries.[1,4]) Concurrently, the original grains elongate and thin with increasing plastic strain, causing a marked increase in the total high-angle boundary area. In torsion, the change in grain shape occurs as a spiraling of the original grains about the torsion axis and a thinning in the direction parallel to the torsion axis. Ultimately, the original grains thin to the point that their thickness is on the order of twice the subgrain size. Grain-boundary "serrations" on opposite sides of the grains begin to come into contact with each other, causing the grains to pinch off.[6] Annihilation of high-angle boundaries results, and the high-angle boundary area remains fixed with increasing strain. Through this mechanism,

G.A. HENSHALL, Metallurgist, is with the Lawrence Livermore National Laboratory, Livermore, CA 94550. M.E. KASSNER, Associate Professor, is with the Mechanical Engineering Department, Oregon State University, Corvallis, OR 97331. H.J. McQUEEN, Professor, is with the Mechanical Engineering Department, Concordia University, Montreal, PQ, Canada.

Manuscript submitted June 3, 1991.

up to one-third of the subgrain facets become high-angle boundaries at very high strains. However, these boundaries have their ancestry in the original grain boundaries; they are not the result of discontinuous or continuous dynamic recrystallization. More detailed descriptions of geometric dynamic recrystallization have been given elsewhere.[4,6,8]

The hot-working behavior of Al-Mg alloys also has been extensively studied.[11–19] However, the dynamic restoration mechanisms (*i.e.*, dynamic recovery, discontinuous dynamic recrystallization, or continuous dynamic recrystallization) are far less clear. Some investigators[14,18] have concluded that increasing the concentration of Mg reduces the SFE and hence dynamic recovery, leading to discontinuous dynamic recrystallization. For alloys with 0 to 4 pct Mg, McQueen *et al.*[5] have speculated that the development of what appears to be a microstructure typical of discontinuous dynamic recrystallization may be caused instead by geometric dynamic recrystallization with dynamic recovery, just as with pure Al. Others have proposed different mechanisms to account for the observed microstructures.[15,16] Some earlier investigations concluded that (presumably discontinuous) dynamic recrystallization had occurred in Al-Mg alloys, because a dislocation substructure within the "recrystallized" grains was observed.[11,12,14] (These observations were made subsequent to deformation within the three-power solute drag regime, in which subgrain formation is suppressed, as well as at temperature-compensated strain rates above those for which three-power behavior occurs.) This conclusion is suspect, however, because the geometric dynamic recrystallization mechanism produces a microstructure that appears very similar, in many aspects, to that produced by discontinuous dynamic recrystallization. Only by careful metallography and transmission electron microscopy (TEM) at progressively larger strains can these mechanisms be distinguished from one another.[5]

The purpose of the present investigation was to study dynamic restoration in an Al-5.8 at. pct Mg alloy deformed in the three-power creep, or "viscous solute drag," regime. Using solid-specimen torsion tests so that large strains could be achieved, the goal was to determine whether large strain dynamic restoration was due to a mechanism like discontinuous dynamic recrystallization or to dynamic recovery with geometric dynamic recrystallization. Deformation conditions were selected to be within the solute drag regime because subgrain formation is suppressed (*i.e.*, subgrains will not form or their formation occurs at relatively large strains). Since subgrain formation is a prerequisite to geometric dynamic recrystallization, three-power deformation is a strong test of whether the microstructures of warm- and hot-worked Al-Mg alloys are a result of this mechanism.

Torsion tests were performed to various strains, up to the failure strain of 10.8, and quenching took place immediately upon the termination of deformation. At each strain, optical microscopy (OM) and TEM were used to characterize the microstructure in terms of grain shape and orientation, network dislocation density (subgrain interior), subgrain size, and sub-boundary misorientation. These results were analyzed to determine the dynamic restoration mechanism that controls the hot-deformation behavior of Al-5.8 at. pct Mg deformed in the solute drag regime. The relationship between the microstructure and the stress *vs* strain behavior also was studied. The results of this investigation, of course, provide insight into the dynamic restoration mechanism occurring in other Al-Mg alloys deforming in the solute drag regime at the present, as well as other, temperatures and strain rates.

II. EXPERIMENTAL PROCEDURES

The Al-5.8 at. pct Mg (5.2 wt pct Mg) alloy, hereafter identified as Al-6Mg, used in this study was obtained as a 76.2-mm-diameter cylindrical casting, with a total impurity level not greater than 5 ppm. A 76-mm-long section from the center of the casting was cut and homogenized by annealing in air at 773 K for 24 hours. The thickness of the casting was reduced by upset forging at 623 K and then warm rolling at 573 K to a final thickness of 15.5 mm. The plate was quenched in oil to ensure that the alloy remained single phase following the final rolling pass. Cylindrical torsion samples with a gage length, L, equal to 25.4 mm and a gage diameter, d, equal to 5.08 mm ($L/d = 5$) were machined from the plate. In addition, several specimens with $L = 25.4$ mm and $d = 2.54$ mm ($L/d = 10$) were machined. Following machining, all of the samples were annealed in vacuum for 1 hour at 723 K and quenched with ambient-temperature argon gas. Transmission electron microscopy observations did not reveal any significant quantity of second-phase particles.

Torsion testing of specimens with $L/d = 5$ was performed on the Stanford torsion machine[20] at 698 K and an equivalent uniaxial strain rate (at the outer fiber) of $1.43 \times 10^{-3}\ s^{-1}$. Figure 1 indicates that these conditions

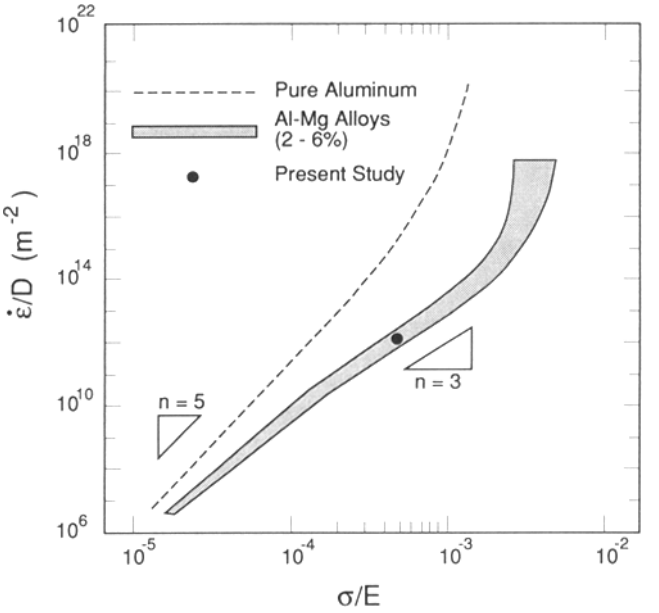

Fig. 1—The diffusion-compensated steady-state strain rate, $\dot{\varepsilon}/D$, as a function of the modulus-compensated steady-state flow stress, σ/E, for pure Al and Al-Mg alloys.[34] The testing conditions used in the present investigation are indicated by the solid circle.

are well within the three-power, or solute drag, regime for this alloy. The specimens were deformed in a high-purity argon atmosphere and automatically water quenched immediately following deformation. Specimens were deformed to equivalent uniaxial strains of approximately 0.18, 1.1, 2.1, 4.3, 9.0, and 10.8 (failure) so that the evolution of the microstructure could be evaluated. The shear stress and shear strain at the outer fiber were calculated using the following classic equations:[21]

$$\bar{\varepsilon} = \frac{1}{\sqrt{3}} \frac{r}{L} \alpha \qquad [1]$$

$$\bar{\sigma} = \sqrt{3} \frac{M}{2\pi r^3} (3 + k + m) \qquad [2]$$

where $\bar{\varepsilon}$ is the equivalent uniaxial strain, r is the radius of the gage section, α is the twist angle, $\bar{\sigma}$ is the equivalent uniaxial stress, M is the torque, k is the strain-hardening exponent (assumed to be zero at steady state or during softening), and m is the strain rate sensitivity (assumed to be 0.3).

Specimens with $L/d = 10$ were tested using a Rheometrics Mechanical (RMS-800)/Dynamic (RDSII) Spectrometer at the temperature and strain rate mentioned previously. This machine, which is usually employed to measure the viscosity of polymers, is highly aligned, allows control of the axial stress to within ±0.2 MPa, and suffers no load cell drift. Therefore, it was used to accurately measure the torque *vs* twist-angle curve of the Al-6Mg alloy.

Optical microscopy was performed on chord sections cut from the 3/4-radius position of the gage section of the quenched torsion specimens. These sections were mechanically polished and then anodized to reveal the grains and subgrains under polarized light. Anodizing was performed using a solution of 4 pct fluoboric acid in water and a high-purity lead cathode, with voltages of approximately 15 to 25 V applied for 3 minutes.

Transmission electron microscopy samples were prepared by spark cutting 3-mm disks normal to the radius from the 3/4-radius position of the torsion specimens. The disks were carefully lapped to a thickness of about 0.5 mm using 600-grit SiC paper. These foils were electrochemically thinned in a solution of 94 pct methanol, 5 pct sulfuric acid, and 1 pct hydroflouric acid using a Struers Tenupol II. The foils were examined with a JEOL 200CX TEM operating at 200 kV utilizing a double-tilt stage. Subgrain size, λ, measurements were made using a line-intercept method, and the dislocation density not associated with subgrain walls, ρ, was measured by counting the number of dislocations intersecting the foil surface. {220} two-beam conditions were used to image the dislocations for the measurement of ρ. The measured ρ was not adjusted for the fact that, on average, one-sixth of the dislocations will satisfy the invisibility condition for these beam conditions. The misorientation angle between adjacent subgrains (or grains), Θ, was determined using the double-tilt stage and by measuring the minimum angle required to bring the lattices of the adjacent subgrains into coincidence. A total of 45 boundaries were measured at each strain level.

III. EXPERIMENTAL RESULTS AND DISCUSSION

A. *Relationship between the Microstructure and the Stress-Strain Curve*

The evolution of the dislocation density within subgrain interiors, subgrain size, and flow stress with large strain deformation is illustrated in Figure 2. As shown in the insert of Figure 2(c), the flow stress rises very rapidly to a peak value of about 37 MPa. It then decreases over a strain of just 0.015 to approximately 25 MPa, where it remains relatively constant up to a strain of about 0.06. This stress of 25 MPa is equivalent to the steady-state stress that would be achieved in the usual tensile test and is consistent with values reported in the literature for similar alloys deforming at similar temperature-compensated strain rates[22,23,24] (Figure 1). The rapid decrease in stress from an initial peak value to the steady-state value was also observed by Usui *et al.*[12] in an Al-3 pct Mg alloy and by Henshall[25] for several binary Al-Mg alloys. This behavior is the constant strain rate equivalent of the inverted primary creep transient often observed during three-power deformation.[22,26,27] It is generally accepted[12,26,28] that the strength is initially high because of the low mobile dislocation density and then decreases due to dislocation multiplication. Since dynamic

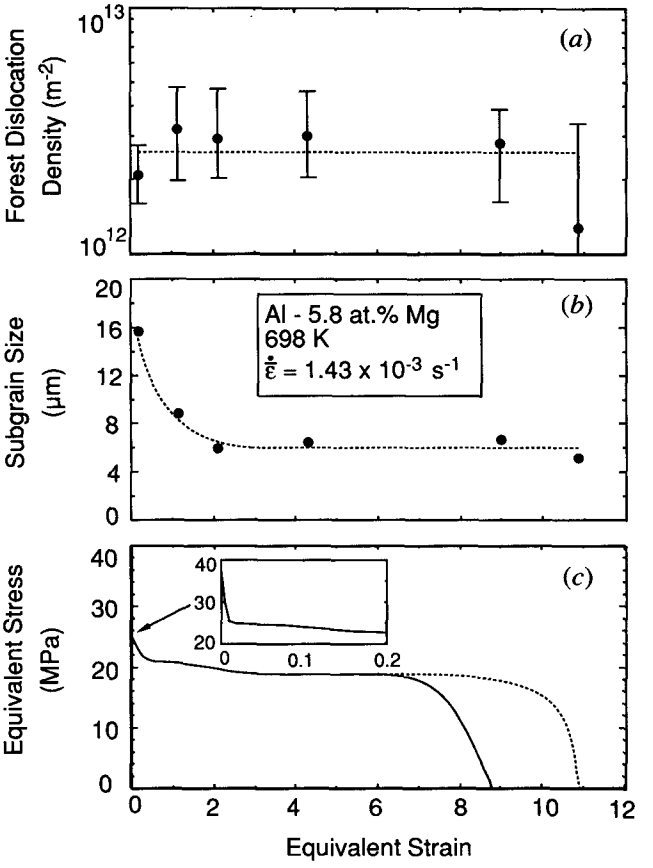

Fig. 2—The evolution of microstructure and stress with large strain deformation of Al-5.8 at. pct Mg deformed in torsion at 698 K and an equivalent uniaxial strain rate of 1.43×10^{-3} s^{-1}. (*a*) The density of dislocations not associated with subgrain walls (forest dislocations), (*b*) the average subgrain size, and (*c*) the equivalent uniaxial stress at the outer fiber as a function of the equivalent uniaxial strain.

restoration at large strains was the focus of the present study, dislocation densities were not measured below $\bar{\varepsilon} = 0.18$. Therefore, this explanation of the transient at $\bar{\varepsilon} \leq 0.015$ cannot be confirmed from the data in Figure 2(a). Figure 2(c) also shows that there is a gradual 24 pct reduction in stress from 25 MPa to approximately 19 MPa over the wide strain range from about 0.06 to 3.5. A similar decrease (about 20 pct) in torsional flow stress has been observed in pure aluminum and was convincingly related to a decrease in the average Taylor factor due to texture development.[4,7] Texture development also appears to be the cause for the decrease in stress from 25 to about 19 MPa shown in Figure 2(c). This decrease in stress is not believed to be caused by discontinuous dynamic recrystallization, in part because the strain range over which it occurs is significantly broader than that observed for materials in which discontinuous dynamic recrystallization causes flow softening, such as Ni and Cu,[9,10] nor do the microstructural observations described later in this section support a discontinuous dynamic recrystallization explanation of this softening. Confirmation of the textural softening hypothesis using X-ray diffraction was beyond the scope of this study. Finally, note that the solid curve in Figure 2(c) represents the behavior of an $L/d = 10$ specimen tested using the Rheometrics Spectrometer. The dashed line represents the increased ductility of the $L/d = 5$ specimens tested on the Stanford torsion machine, from which microstructural data were extracted. The torsional ductility of 10.8 is consistent with that obtained by Ueki *et al.*[18] for a similar alloy deforming under similar conditions.

Figure 2(a) shows that for strains between 0.18 and failure, the density of dislocations not associated with subgrain boundaries is essentially constant. The steady-state density, ρ_{ss}, of about 3×10^{12} m^{-2} is consistent with values reported by Matsuno and Oikawa[22] and by Orlová and Cadek[29] for similar Al-Mg alloys deforming in the three-power creep regime at stresses similar to that reported here.

Based upon tensile creep experiments, several investigators[23,24] have suggested that subgrains do not form in Al-Mg alloys deformed in the solute drag regime, although some more recent evidence for subgrain formation has been presented.[16,27,30,31] The reason for this controversy apparently lies in the sluggishness of the subgrain development within grain interiors. As shown in Figures 3(a) and (b), at $\bar{\varepsilon} = 0.18$, the subgrain boundaries form only near the original high-angle grain boundaries; there is an absence of subgrains in the grain interiors. Weckert and Blum[30] made a similar observation for an Al-5 pct Mg alloy deforming at a diffusion-compensated strain rate of 1×10^{13} m^{-2}, which is at the high stress end of the solute drag regime (Figure 1). In addition, the sub-boundaries formed at low strains near the original grain boundaries are often fragmented and may not completely form a subgrain. The initial formation of subgrains only near the original grain boundaries produces a microstructure similar to the "core and mantle" structure observed by Humphreys and Drury[15] and Drury and Humphreys.[16] The present study shows that well-established subgrains do not appear throughout the original grains until a strain on the order of 1 is attained. This explains why investigations utilizing tensile tests that were carried only to the inception of steady state did not conclusively reveal subgrain formation. Figures 3(c) and (d) clearly show that well-developed subgrains form within grain interiors at large strains for the three-power deformation conditions employed in the present investigation. Drury and Humphreys[16] came to a similar conclusion in their study of an Al-5 pct Mg alloy deformed in compression in the solute drag regime.

The evolution of the subgrains during large strain deformation in the solute drag regime is quantified in Figures 2(b), 4, and 5. Figure 2(b) shows that subgrain refinement occurs up to an equivalent uniaxial strain of about 2 (well beyond that for which ρ_{ss} is reached), with the steady-state diameter, λ_{ss}, being about 6 μm. Interestingly, this value of λ_{ss} is about the same as that observed[32] for pure aluminum deformed at the steady-state stress observed in the present investigation (25 MPa). In pure Al, however, λ_{ss} is reached by $\bar{\varepsilon} \approx 0.2$.[1] The histograms of boundary misorientation angle as a function of strain (Figure 4) reveal that the subgrain boundary structure is also evolving at strains well above that for which ρ_{ss} is reached. This point is emphasized in Figure 5, which shows that the average misorientation angle across subgrain boundaries that form from dislocation reaction increases from about 0.46 deg at a strain of 0.18 to a saturated value of about 1.6 deg at a strain of 2.1. The observation of an eventual saturation in misorientation across sub-boundaries that form by dislocation reaction is consistent with the work of Kassner and McMahon[1] on pure Al. The results are also consistent with those of McQueen and co-workers[6,7,8] on pure Al, which showed that sub-boundaries of 1 to 2 deg were common at strains up to 60, although some deformation bands of 6 to 8 deg had developed. The saturation of Θ at large strains observed in these previous studies and in the present work emphasizes the limitation of tensile tests performed only to low strains, in which saturation of Θ often is not observed.[33] The data in Figure 5 also shed doubt on the conclusion of Orlová and Cadek[29] that Θ for Al-5 pct Mg deformed in the solute drag regime reaches a peak at moderately low strains, ~0.15, and then decreases with further straining; this conclusion was based on low strain tensile data.

Figure 2 clearly shows that the flow stress does not increase (but decreases, presumably due to textural softening) during the refinement of the subgrains. In addition, as Θ increases, implying a refinement of the dislocation structure within subgrain walls, the flow stress decreases somewhat. Figures 2(c) and 5 clearly show that the saturation of Θ is independent of the flow stress.* It therefore appears that the subgrains are not an important substructural feature in determining the flow stress of Al-Mg alloys in the three-power creep regime. Raghavan

*This behavior was also observed in pure Al by Kassner and McMahon,[1] in which Θ saturated at a somewhat lower strain, about 1, and reached a slightly lower saturated value, about 1.2 deg. The saturation of Θ at a larger value for the alloy than for pure Al is consistent with the observation of Weckert and Blum (Fig. 4 of Ref. 30) that there is an increase in the saturated value of Θ as the flow stress increases.

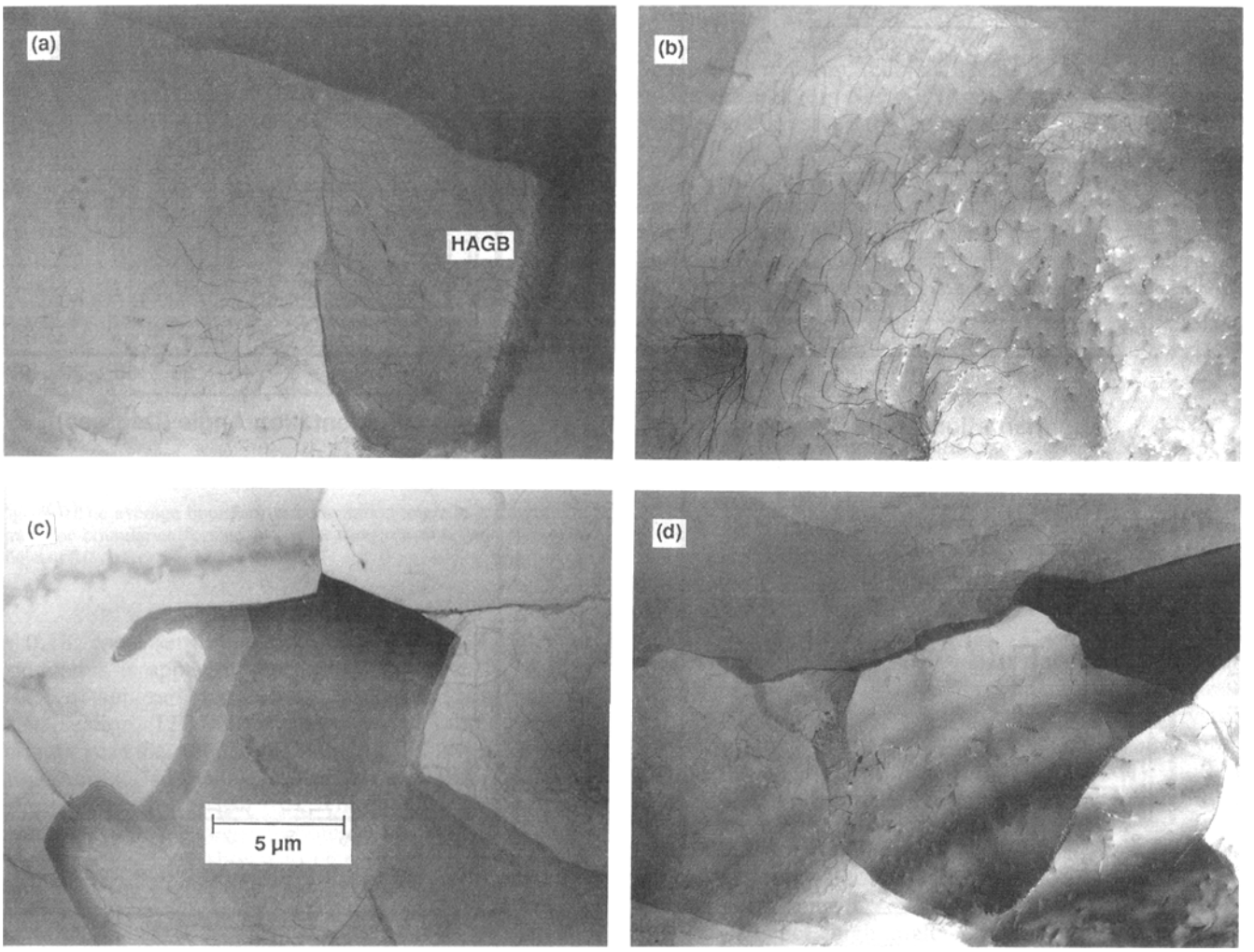

Fig. 3—Bright-field TEM micrographs of Al-5.8 at. pct Mg deformed at 698 K and a strain rate of 1.43×10^{-3} s^{-1}: (*a*) $\bar{\varepsilon} = 0.18$, near a high-angle grain boundary (HAGB); (*b*) $\bar{\varepsilon} = 0.18$, grain interior; (*c*) $\bar{\varepsilon} = 1.1$, grain interior; and (*d*) $\bar{\varepsilon} = 9.0$, grain interior.

and Shapiro[13] reached the same conclusion in their study of Al-4 pct Mg under a variety of deformation conditions.

B. *Geometric Dynamic Recrystallization*

Evidence to support the hypothesis that geometric dynamic recrystallization is occurring in Al-6Mg deformed in the solute drag regime is given by the histograms in Figure 4. Due to the relatively large starting grain size of about 410 μm, the chances of observing an original high-angle grain boundary (Θ generally greater than about 10 deg) in the transparent region of a TEM foil are initially fairly small (Figures 4(a) through (c)). By a strain of 4.3, however, about 10 pct of the subgrain boundaries have misorientations greater than 10 deg and by a strain of 10.8 this value exceeds 20 pct. This increase in the fraction of high-angle boundaries is consistent with the thinning of grains that precedes their pinching off in the manner characteristic of geometric dynamic recrystallization. At the highest strains, the histograms in Figure 4 evince a bimodal character similar to that observed by Kassner and co-workers[1,4] for ultralarge strain deformation of pure Al. That is, at large strains where geometric dynamic recrystallization is complete (or nearly complete), there are two populations of subgrain facets. One population consists of boundaries that form from dislocation reaction, as with subgrain boundaries formed during low strain creep. The misorientation across these typically is between 0 and 6 deg with an average of about 2 deg. The other population consists of the *original* high-angle boundaries and, as with pure Al,[1] has misorientations that vary between about 10 and 60 deg with an average Θ of about 35 deg. According to the description of geometric dynamic recrystallization given in Section I, the fraction (or area) of these high-angle boundaries increases as the original grains thin with increasing strain. The bimodal character of the histograms, therefore, becomes more apparent at the larger strains.

The evolution of the boundary misorientation histograms toward a bimodal shape also was cited as evidence that geometric dynamic recrystallization, rather than a continuous dynamic recrystallization mechanism, occurs in pure aluminum.[1,4,6,8] As concluded in these investigations, if the increase in the fraction of high-angle boundaries with increasing strain was produced by a continuous increase in the misorientation angle of subgrain

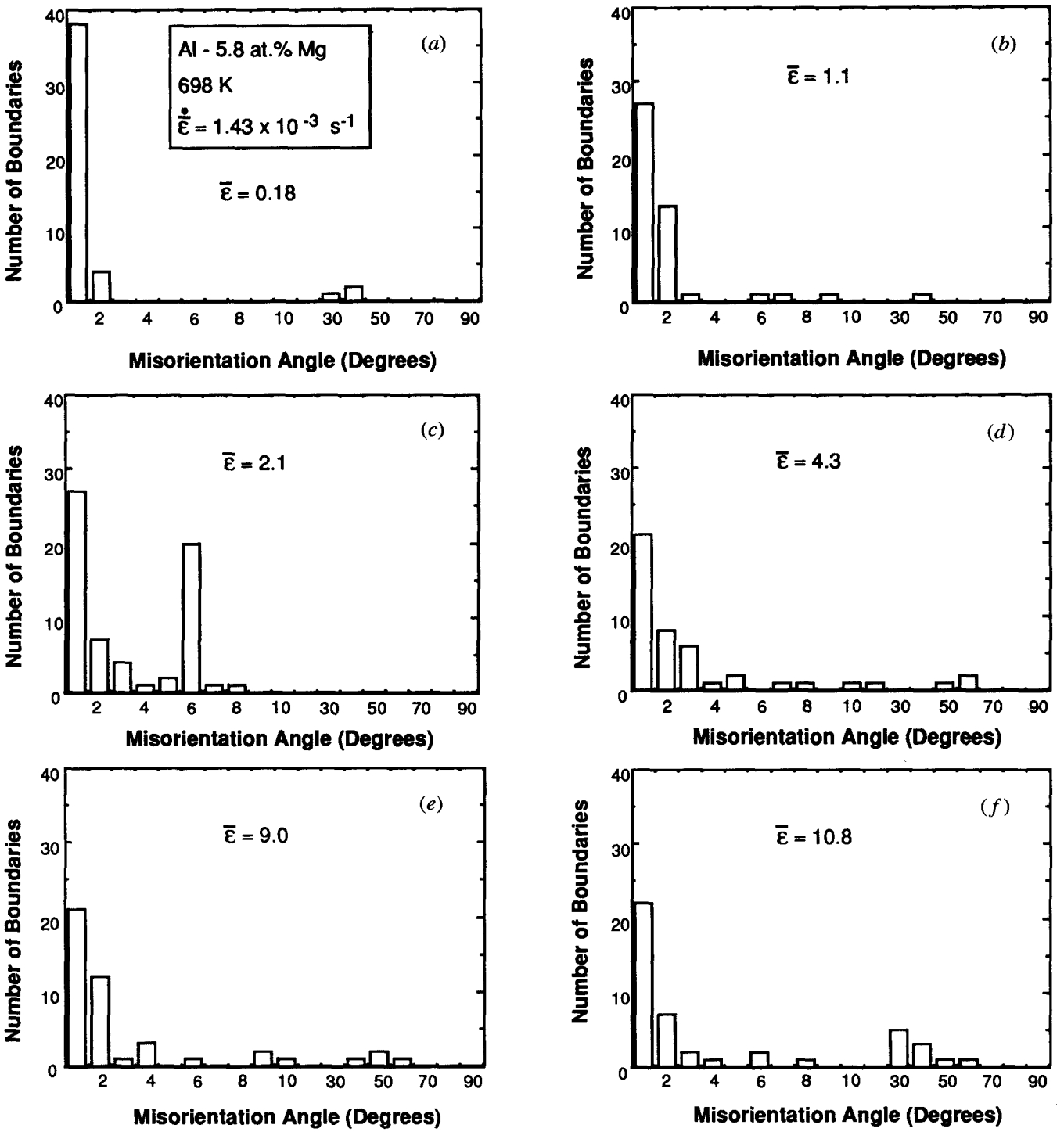

Fig. 4—(*a*) through (*f*) Frequency/misorientation-angle histograms of boundaries formed in Al-5.8 at. pct Mg specimens deformed to the indicated equivalent uniaxial strains. Note the change in the scale of the abscissa at 10 deg. Forty-five boundaries were measured at each strain.

boundaries formed by dislocation reaction, a continuous rise in Θ with $\bar{\varepsilon}$ would be expected. By contrast, geometric dynamic recrystallization is characterized by the evolution of a bimodal distribution representing two distinct populations of boundaries. The data in Figure 4 clearly support the view that geometric, not continuous, dynamic recrystallization is responsible for the microstructural changes occurring in Al-6Mg deformed in the solute drag regime. The data in Figure 5 showing the saturation of the misorientation angle of boundaries formed by dislocation reaction are consistent with this conclusion as well.

Optical microscopy of the deformed torsion samples also supports the geometric dynamic recrystallization hypothesis of microstructural evolution. Figure 6 shows optical micrographs of tangential sections taken from the 3/4-radius position of the torsion specimens, with the torsion axis horizontal in each micrograph. At a strain

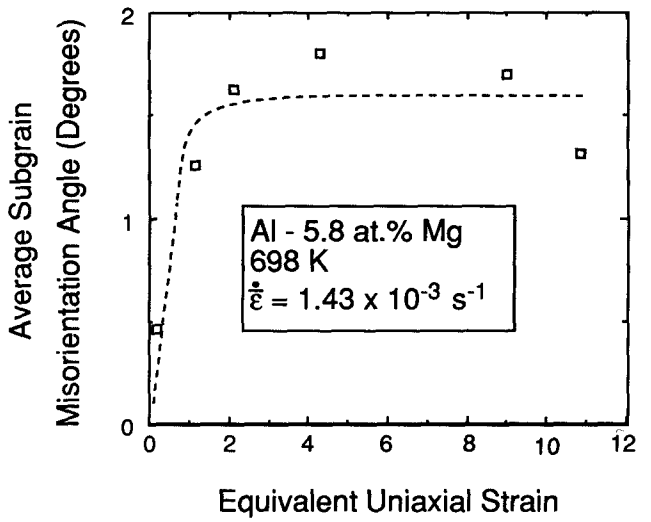

Fig. 5—The average boundary misorientation angle as a function of strain for boundaries formed by dislocation reaction (misorientation angle of 10 deg or less).

of 0.18, some serrating of the original high-angle grain boundaries is apparent, but otherwise, there is no evidence of subgrain formation. As discussed in the previous section, TEM observations reveal sub-boundaries forming near the original high-angle grain boundaries and an absence of subgrain boundaries in the interior of the grains (Figures 3(a) and (b)). The junction of low misorientation ($\Theta < 2$ deg) sub-boundaries and a high-angle boundary has been shown to cause triple points or serrations of the high-angle boundary.[1] As the strain increases, the original grains spiral around the torsion axis and the high-angle boundary area increases. This is observable as a change in the grain shape from equiaxed to one in which the grains are elongated and increasingly perpendicular to the torsion axis (Figures 6(c) and (d)). The narrowing of the grains also is observable. Although more discernable with TEM (Figure 3) rather than OM, an increased incidence of sub-boundaries forming from dislocation reaction is evident in Figure 6 as the strain increases. It is noteworthy that the micrographs in Figure 6 are remarkably similar to those presented by Kassner and co-workers[1,4] of pure Al, for which geometric dynamic recrystallization was confirmed. Finally, neither OM nor TEM examination provided any evidence of strain-free grains growing from a region that previously showed a high dislocation density. Such an observation could be expected if discontinuous dynamic recrystallization were occurring.

The work of Humphreys and Drury[15] and Drury and Humphreys[16] supports the findings of the present investigation. They performed compression tests on an Al-5 pct Mg alloy at temperatures and strain rates comparable to those used in this study. The tests were performed to strains of only about 1.5, and hence, the analyses were restricted to lower strain levels. These investigators emphasized the development of sub-boundaries, some of which have high ($\Theta > 10$ deg) misorientations, in the vicinity of the original grain boundaries. These local details were not the principal focus of our work. The key point is that Drury and Humphreys acknowledged that their large-strain specimens showed evidence of development toward geometric dynamic recrystallization.

As discussed in Section I, geometric dynamic recrystallization involves the spiraling of the original grains around the torsion axis. This causes the grains to thin in the direction parallel with the torsion axis, until ultimately they are on the order of twice the subgrain size. At this point, the "pinching off" of the serrated grain boundaries[5,6] establishes a steady-state number (or area) of high-angle boundaries. The relationship describing the thinning of the original grains as the strain increases is[8]

$$d_{ga} = \frac{d_{go}}{\sqrt{3}\,\bar{\varepsilon}} \qquad [3]$$

where d_{go} is the original grain size and d_{ga} is the reduced axial width of the grains at the equivalent uniaxial strain of $\bar{\varepsilon}$. From Eq. [3], the "critical" strain, $\bar{\varepsilon}_c$, required to reach the point at which $d_{ga} \approx 2\lambda$ is given by

$$\bar{\varepsilon}_c = \frac{d_{go}}{2\sqrt{3}\,\lambda} \qquad [4]$$

For the Al-6Mg alloy, $d_{go} \approx 410\ \mu m$ and $\lambda_{ss} \approx 6\ \mu m$ (Figure 2). Equation [4], therefore, predicts a critical strain of about 19.7 to complete geometric dynamic recrystallization. Due to the limited torsional ductility of Al-6Mg under the conditions tested, this strain could not be reached. Equation [3] does predict, however, that at a strain of 10.8, d_{ga} should be 22 μm, which is about 4λ. Therefore, we would expect to view roughly half of the concentration of high-angle boundaries that would occur at complete geometric dynamic recrystallization, or about 15 to 20 pct high-angle boundaries. The data in Figure 4(f) show that roughly 20 pct of the sub-boundaries have misorientation angles greater than 10 deg at the strain of 10.8, which is consistent with the geometric dynamic recrystallization model. In addition, the microstructures in Figures 6(d) through (f) are very similar to those observed in pure Al[1,6–8] prior to the completion of geometric dynamic recrystallization.

Since only one set of deformation conditions was used in the present work, further studies of Al-Mg alloys could include higher strain rates. An increased tendency toward discontinuous dynamic recrystallization may be expected in this case. Testing at lower temperatures also would be useful. Combined with the results of the present study, such tests would determine the restoration mechanism over more general temperature and strain rate conditions. Unfortunately, performance of these experiments and the required microstructural analyses was beyond the scope of this investigation.

IV. SUMMARY AND CONCLUSIONS

Elevated-temperature torsion tests have been used to study the mechanism of dynamic restoration in an Al-5.8 at. pct Mg (5.2 wt pct Mg) alloy deformed in the solute drag regime. Analyses of the stress-strain curve and the microstructural evolution (grain shape and orientation, dislocation density, subgrain size, and boundary misorientations) led to the following conclusions.

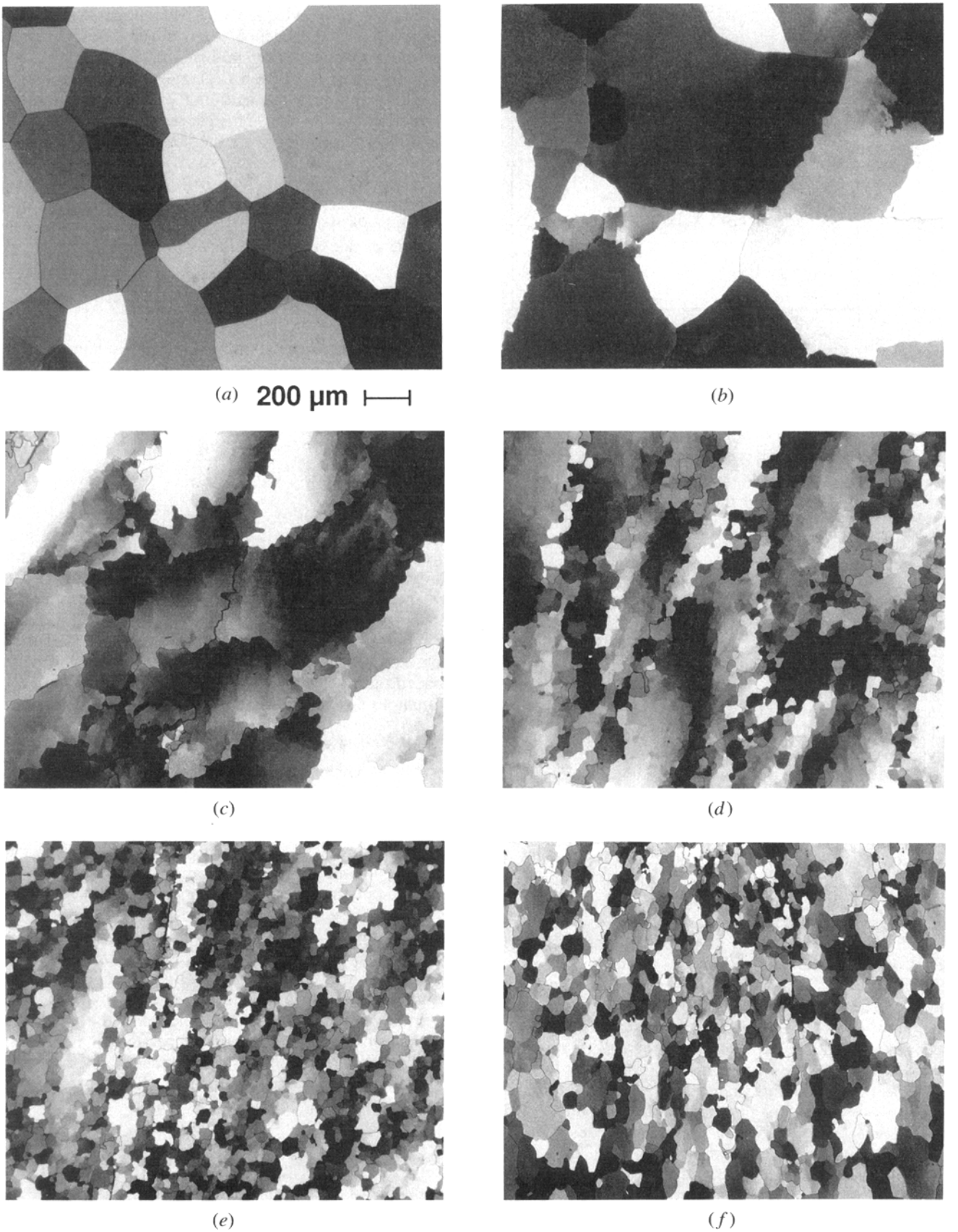

Fig. 6—Optical micrographs of chord sections taken from the 3/4-radius position of the Al-5.8 at. pct Mg torsion specimens deformed to outer-fiber equivalent uniaxial strains of (*a*) 0.0, (*b*) 0.18, (*c*) 1.1, (*d*) 2.1, (*e*) 4.3, and (*f*) 9.0. The torsion axis is horizontal in each micrograph. In (f), the grains at the top of the micrograph, which are near the outer fiber of the torsion specimen, appear to be narrower than those at the bottom of the micrograph, which are nearer to the 3/4-radius position. The difference is due to the gradient in strain and the geometry of the grains.

1. Dynamic restoration occurs through dynamic recovery, which gives rise to geometric dynamic recrystallization in a manner very similar to that already established for pure aluminum.[1,2,4–8] Together with the previous work on pure aluminum, this suggests that geometric dynamic recrystallization occurs in materials with a high SFE when the grains thin to about double the subgrain diameter.
2. No evidence was found for discontinuous dynamic recrystallization, thus indicating that dynamic recovery is not sufficiently reduced by additions of Mg to Al up to 5.8 at. pct, at least in the solute drag regime.
3. Although they form more slowly than in pure aluminum, equiaxed subgrains eventually form in Al-5.8 at. pct Mg deformed in the solute drag regime. This process begins at the original high-angle grain boundaries and then spreads to the grain interiors. The steady-state subgrain size for the conditions tested is approximately 6 μm, and the misorientation angle of these boundaries, which form from dislocation reaction, saturates at about 1.6 deg. During the evolution of the subgrains toward saturation at an equivalent uniaxial strain of about 2, the flow stress decreases slightly, suggesting that the subgrains do not significantly influence the strength.

ACKNOWLEDGMENTS

The authors thank M. Wall of the Lawrence Livermore National Laboratory (LLNL) for performing the TEM and B. Kershaw of LLNL for the optical metallography. Torsion testing with the Rheometrics Spectrometer by N. Nguyen of LLNL is also gratefully acknowledged. Work by one of the authors (GAH) was performed under the auspices of the United States Department of Energy under Contract No. W-7405-ENG-48 at LLNL.

REFERENCES

1. M.E. Kassner and M.E. McMahon: *Metall. Trans. A*, 1987, vol. 18A, pp. 835-46.
2. M.E. Kassner: *Metall. Trans. A*, 1989, vol. 20A, pp. 2182-85.
3. M.E. Kassner, N.Q. Nguyen, G.A. Henshall, and H.J. McQueen: *Mater. Sci. Eng.*, 1991, vol. A132, pp. 97-105.
4. M.E. Kassner, M.M. Myshlyaev, and H.J. McQueen: *Mater. Sci. Eng.*, 1989, vol. A108, pp. 45-61.
5. H.J. McQueen, E. Evangelista, and M.E. Kassner: *Z. Metallkd.*, 1991, vol. 82, pp. 336-45.
6. J.K. Solberg, H.J. McQueen, N. Ryum, and E. Nes: *Phil. Mag. A*, 1989, vol. 60A, pp. 447-71.
7. H.J. McQueen, J.K. Solberg, N. Ryum, and E. Nes: *Phil. Mag. A*, 1989, vol. 60A, pp. 473-85.
8. H.J. McQueen, O. Knustad, N. Ryum, and J.K. Solberg: *Scripta Metall.*, 1985, vol. 19, pp. 73-78.
9. H.J. McQueen and J.J. Jonas: *J. Appl. Metalwork*, 1984, vol. 3, pp. 233-41.
10. H.J. McQueen and J.J. Jonas: *J. Appl. Metalwork*, 1984, vol. 3, pp. 410-20.
11. E. Usui, T. Inaba, and N. Shinano: *Z. Metallkd.*, 1986, vol. 77, pp. 684-93.
12. E. Usui, T. Inaba, and N. Shinano: *Z. Metallkd.*, 1986, vol. 77, pp. 179-87.
13. M. Raghavan and E. Shapiro: *Metall. Trans. A*, 1980, vol. 11A, pp. 117-21.
14. K.J. Gardner and R. Grimes: *Met. Sci.*, 1979, vol. 13, pp. 216-22.
15. F.J. Humphreys and M.R. Drury: *Aluminum Technology*, T. Sheppard, ed., Institute of Metals, London, 1986, pp. 191-96.
16. M.R. Drury and F.J. Humphreys: *Acta Metall.*, 1986, vol. 34, pp. 2259-71.
17. T. Sheppard, M.B. Tutcher, and H.M. Flower: *Met. Sci.*, 1979, vol. 13, pp. 473-81.
18. M. Ueki, S. Horie, and T. Nakamura: *Aluminum Alloys Physical and Mechanical Properties*, E.A. Starke and T.H. Sanders, eds., EMAS, Warley, U.K., 1986, pp. 419-22.
19. X.Y. An, J.P. Lin, T.C. Lei, and B.T. Yu: *Strength of Metals and Alloys*, P.O. Kettunen, T.K. Lepisto, and M.E. Lehtonen, eds., Pergamon Press, Oxford, 1989, vol. 2, pp. 971-76.
20. C.M. Young and O.D. Sherby: *Metal Forming: Interpretation between Theory and Practice*, A.L. Hoffmanner, ed., Plenum Press, New York, NY, 1971, p. 429.
21. D.S. Fields and W.A. Backofen: *Proc. ASTM*, 1957, vol. 57, p. 1259.
22. N. Matsuno and H. Oikawa: *Scripta Metall.*, 1981, vol. 15, pp. 319-22.
23. P. Yavari and T.G. Langdon: *Acta Metall.*, 1982, vol. 30, pp. 2181-96.
24. P. Yavari, F.A. Mohamed, and T.G. Langdon: *Acta Metall.*, 1981, vol. 29, pp. 1495-1507.
25. G.A. Henshall: Ph.D. Dissertation, Stanford University, Stanford, CA, 1987.
26. H. Oikawa, K. Honda, and S. Ito: *Mater. Sci. Eng.*, 1984, vol. 64, pp. 237-45.
27. M.J. Mills, J.C. Gibeling, and W.D. Nix: *Acta Metall.*, 1985, vol. 33, pp. 1503-14.
28. W.D. Nix and B. Ilschner: *Strength of Metals and Alloys*, P. Haasen, V. Gerold, and G. Kostorz, eds., 1979, pp. 1503-30.
29. A. Orlová and J. Cadek: *Z. Metallkd.*, 1974, vol. 65, pp. 200-04.
30. E. Weckert and W. Blum: *Strength of Metals and Alloys*, H.J. McQueen, J.-P. Bailon, J.I. Dickson, J.J. Jonas, and M.G. Akben, eds., Pergamon Press, Oxford, 1985, pp. 773-78.
31. L. Ivanchev and D. Chevdarova: *Plasticity and Resistance to Metal Deformation*, S. Blecic, ed., University of Titograd, Titograd, Yugoslavia, 1986, pp. 348-61.
32. T.J. Ginter and F.A. Mohamed: *J. Mater. Sci.*, 1982, vol. 17, pp. 2007-12.
33. M.A. Morris and J.L. Martin: *Acta Metall.*, 1984, vol. 32, pp. 549-61.
34. T.R. McNelly, D.J. Michel, and A. Salama: *Scripta Metall.*, 1989, vol. 23, pp. 1657-62.